World Journal of Advanced Engineering Technology and Sciences
eISSN: 2582-8266
Cross Ref DOI: 10.30574/wjaets
Journal homepage: https://wjaets.com/

(REVIEW ARTICLE)

Check for updates

Sedimentological investigation of mining pollutants in watersheds using core sampling techniques: A case study of Tar Creek, Oklahoma, USA

Agboro Harrison [1,*] and Sandra Isioma Erue [2]

[1] *Department of Environmental Health and Management, University of New Haven, West Haven, CT., USA. 06516.*
[2] *Department of Environmental and Interdisciplinary Sciences, Texas Southern University, Houston, TX., USA. 77004.*

World Journal of Advanced Engineering Technology and Sciences, 2023, 09(02), 406-416

Publication history: Received on 09 July 2023; revised on 25 August 2023; accepted on 28 August 2023

Article DOI: https://doi.org/10.30574/wjaets.2023.9.2.0237

Abstract

This study investigates the vertical and spatial distribution of heavy metal pollutants in sediment cores collected from the Upper Tar Creek, an ecologically sensitive watershed impacted by lead-zinc mining in southeastern United States. Using stratified core sampling at three transect sites, the analysis focused on the concentrations of Pb, Zn, Cd, As, and Mn, alongside grain size distribution and organic matter content. Results revealed significant surface enrichment of Pb, Zn, Cd, and As, especially at the downstream site, suggesting recent anthropogenic deposition. In contrast, Mn showed increasing concentrations with depth, indicating geogenic input. Strong correlations were observed between metal concentrations, silt-dominated grain size fractions, and elevated loss-on-ignition (LOI) values, highlighting the role of fine, organic-rich sediments in metal retention. Pollution indices (Igeo, EF, CF, and PLI) confirmed substantial contamination, with Site C representing a critical depositional sink. The findings underscore the urgent need for sediment management strategies and contribute a replicable model for sedimentological assessment of mining-impacted river systems in tropical environments.

Keywords: Sediment Core; Heavy Metals; LOI; Grain Size; Pollution Indices; Upper Tar Creek; Mining Impact; Environmental Geochemistry

1. Introduction

The escalation of mining activities across the United States—particularly legacy lead-zinc extraction zones—has resulted in widespread disruption of freshwater ecosystems, especially in sediment-laden rivers that intersect historical mining belts. These operations contribute to the accumulation of heavy metals in riverine sediments, which act as both long-term sinks and secondary sources of environmental contaminants, posing significant risks to ecological integrity and human health (Ali et al., 2022; Herbert & Vepraskas, 2018).

In the Tri-State Mining District, encompassing parts of northeastern Oklahoma, southeastern Kansas, and southwestern Missouri, the Picher–Treece corridor has long been a hub of intensive mineral extraction. The nearby Tar Creek has received decades of runoff and leachate from abandoned mine tailings, traversing semi-rural residential and agricultural zones before joining the Neosho River system (USGS, 2018; Nash & Fey, 2012). While prior investigations have documented surface water contamination and topsoil pollution in this region, sediment cores remain underutilized for reconstructing historical pollutant accumulation across vertical depositional layers.

Sediment cores serve as temporal archives of environmental change, capturing both legacy and contemporary pollution signals (Appleby, 2001). Because of the strong affinity between heavy metals, fine particles, and organic matter, depth-structured geochemical profiling enables the reconstruction of sedimentation rates, pollutant persistence, and the

* Corresponding author: Agboro Harrison.

timing of contamination events (Bai et al., 2020; Zhang et al., 2021). Metals such as Pb, Zn, Cd, Mn, and As are particularly stable in sediment matrices under variable redox conditions, underscoring the need for stratified assessments of their distribution and mobility (MacDonald et al., 2000; Wang et al., 2022).

This study applies multi-core sediment sampling and vertical geochemical analysis to investigate the spatial and depth-dependent distribution of heavy metals in the Upper Tar Creek watershed. By incorporating granulometric data and organic matter content (via loss-on-ignition), the research evaluates the physical-chemical conditions governing contaminant partitioning and mobility. The study also delineates geochemical hotspots and infers anthropogenic sources responsible for legacy sediment contamination.

Given the historical and ongoing use of Tar Creek for domestic, agricultural, and recreational purposes by nearby communities, the findings contribute essential baseline data for environmental remediation planning and watershed risk management. Additionally, this study strengthens the broader U.S. literature on sediment geochemistry in legacy mining regions and addresses the persistent gap in vertically resolved pollutant records across sediment cores.

2. Geological and Hydrological Context

The Upper Tar Creek watershed is located within the northeastern portion of Ottawa County, Oklahoma, part of the Tri-State Mining District (TSMD), which extends into southeastern Kansas and southwestern Missouri. This region is geologically significant due to its extensive lead-zinc mineralization within the Mississippian-age Boone Formation, which consists primarily of cherty limestones interbedded with shales and dolostones. These sedimentary units are heavily fractured and faulted, hosting hydrothermal ore deposits that have historically been exploited through both underground and surface mining. The geologic composition of the watershed plays a critical role in shaping background metal concentrations, sediment mineralogy, and the long-term mobility of contaminants.

Topographically, the watershed features low to moderate relief, with elevations ranging from approximately 210 to 360 meters above sea level. The area experiences a humid subtropical climate, with precipitation distributed fairly evenly throughout the year, averaging around 1,100 to 1,200 mm annually. Seasonal rainfall variability influences both surface runoff and sediment transport, with higher sediment loading typically occurring during spring and early summer due to intense convective storms and snowmelt-driven overland flow.

Hydrologically, Tar Creek originates near the outskirts of the historic mining area and flows eastward, intersecting several zones of active remediation and abandoned tailings piles. The watershed drains a mix of karstified limestone terrain and legacy mining landscapes, where unlined chat piles, open shafts, and smelter remnants contribute to ongoing metal leaching. Its tributaries transport fine-grained sediments enriched with heavy metals, particularly during high-discharge events. The stream exhibits flashy flow characteristics typical of semi-confined watersheds, with rapid discharge increases during storm events followed by low base flow periods that favor contaminant deposition.

Historically, both mechanized mining and ore beneficiation processes discharged untreated tailings and process waters directly into Tar Creek and its tributaries. These discharges contributed metals in both dissolved and particulate-bound forms. During low-flow periods, sedimentation dominates, enabling the vertical accumulation of contaminated layers in depositional zones. Conversely, during storm surges, channel scouring and sediment resuspension alter stratigraphic profiles and promote downstream transport of legacy contaminants.

The interaction between regional geology, fluvial hydrodynamics, and legacy mining infrastructure renders the Upper Tar Creek watershed an important site for examining metal sequestration in sediments. This geologic-hydrologic framework provides the foundation for interpreting vertical metal gradients in sediment cores and for assessing the long-term environmental legacy of intensive mineral extraction in midwestern U.S. River systems.

3. Materials and Sampling Protocol

Sediment sampling was conducted during the late winter and early spring period to maximize accessibility to low-flow sections of the Tar Creek. Three core sampling sites were selected along a longitudinal transect—Upstream (Site A), Midstream (Site B), and Downstream (Site C)—to capture the spatial variability in contaminant deposition driven by hydrodynamic and geomorphologic factors within the watershed. Site selection prioritized fine-grained depositional zones with low turbulence and visible sediment accumulation. All sites were geo-referenced using a high-sensitivity handheld GPS (Garmin eTrex 32x).

At each site, undisturbed sediment cores were extracted using a custom-fabricated PVC push corer (5 cm inner diameter, 50 cm length), manually inserted into the sediment bed to preserve vertical integrity. After retrieval, cores were sealed at both ends, labeled, and placed in ice-cooled containers for transport to the laboratory. In the lab, each core was sectioned into six vertical strata at 5 cm intervals (0–5 cm, 5–10 cm, 10–15 cm, 15–20 cm, 20–25 cm, and 25–30 cm) to enable fine-scale geochemical profiling.

Samples were air-dried at ambient laboratory temperature, gently disaggregated, and sieved through a 2 mm stainless steel mesh to remove gravel and organic debris. Homogenized subsamples were ground to fine powder using an agate mortar and stored in airtight containers. Heavy metal concentrations of lead (Pb), zinc (Zn), cadmium (Cd), manganese (Mn), and arsenic (As) were analyzed using Inductively Coupled Plasma Mass Spectrometry (ICP-MS) following microwave-assisted acid digestion (EPA Method 3052) with a HNO_3–$HClO_4$–HF digestion matrix.

To ensure analytical rigor, quality control procedures included:

- Use of Standard Reference Materials (SRM 2709a, San Joaquin Soil),
- Procedural blanks,
- Triplicate analyses to assess precision and reproducibility.

Grain size distribution was determined using a Malvern Mastersizer 3000 laser particle analyzer after pre-treatment with 30% hydrogen peroxide to remove organic matter and 5% sodium hexametaphosphate as a dispersant. Organic content was quantified via Loss on Ignition (LOI) at 550°C for four hours, providing insight into the organic matter-metal interaction and binding potential within the sediment matrix.

All geochemical, granulometric, and LOI datasets were processed using OriginPro 2022 for statistical summaries and ArcGIS Pro 3.2 for spatial visualization and trend interpolation. This multi-tiered sampling and analysis protocol supports a detailed understanding of sediment-associated contaminant dynamics, particularly across depth gradients, and strengthens the interpretation of depositional histories and anthropogenic impacts within the Tar Creek watershed.

4. Results and Observational Trends

The core sediment samples extracted from the Upper Tar Creek revealed distinct stratigraphic variations in both physical and geochemical properties across the three sampling sites. Visual observations during core sectioning showed a gradational color shift from brownish-gray (0–10 cm) to darker gray and blackish tones at greater depths, indicative of increasing organic content and possible anoxic conditions. Figure 1 captures the visual appearance of sediment core layers across the three sampling sites.

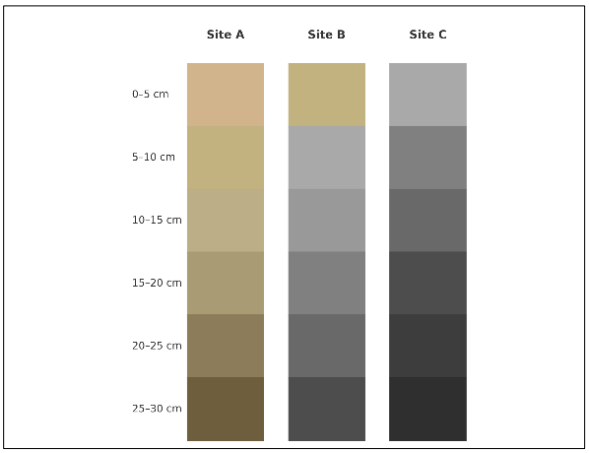

Figure 1 Visual Stratigraphy of Sediment Core Layers (Site A–C). This diagram presents the sediment core profiles for Sites A (Upstream), B (Midstream), and C (Downstream). Each bar is color-graded by depth, illustrating observed variations in sediment color and potential organic content. Site A exhibits more oxidized, lighter sediments; Site B shows transitional layering; while Site C displays darker, organic-rich upper layers indicative of depositional accumulation and reduced redox conditions

4.1. Vertical Distribution of Heavy Metals

Heavy metal concentrations displayed consistent enrichment in the upper 10 cm layers at all sites, with declining values observed at deeper horizons. Figure 2 illustrates the vertical distribution profiles of lead (Pb), zinc (Zn), arsenic (As), cadmium (Cd), and manganese (Mn) across Sites A, B, and C. Pb concentrations were highest at Site C, reaching 228.4 mg/kg in the 0–5 cm layer, followed by 189.7 mg/kg and 164.2 mg/kg at Sites B and A respectively. Similar patterns were observed for Zn and As, both showing sharp declines with depth.

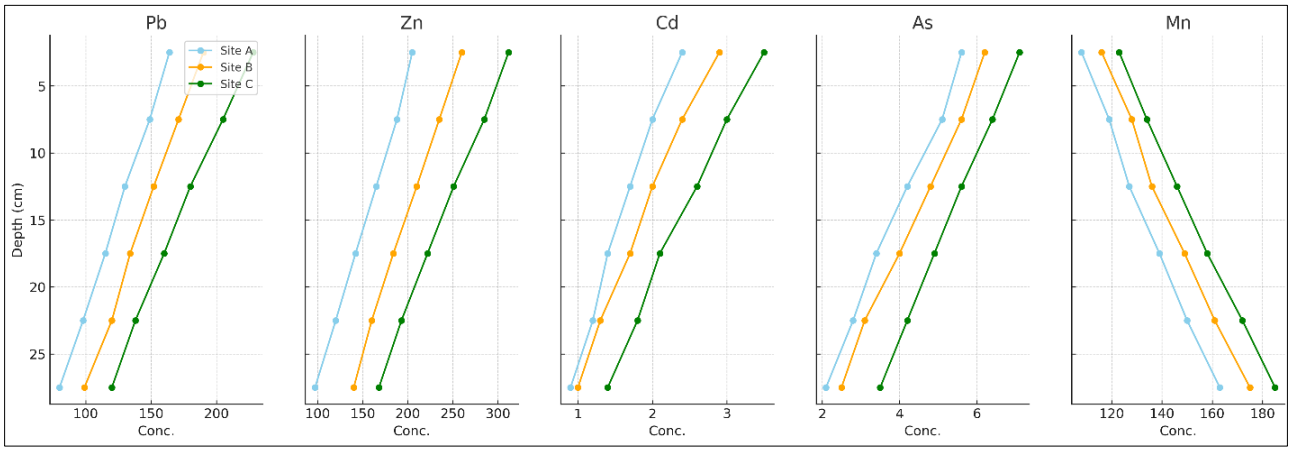

Figure 2 Vertical Distribution Profiles of Heavy Metals by Site. This figure illustrates the depth-specific concentration trends of five heavy metals—Pb, Zn, Cd, As, and Mn—across the three sampling locations in the Upper Tar Creek. Pb, Zn, As, and Cd show higher concentrations in the upper 0–10 cm layers, indicating recent anthropogenic input. Manganese (Mn), by contrast, increases with depth, suggesting remobilization from geogenic sources or deeper sediment zones

In contrast, Mn showed increasing concentration trends with depth, especially at Site A, suggesting post-depositional remobilization from deeper strata or natural lithogenic sources. Table 1 presents summary statistics of metal concentrations by depth and site, emphasizing the relative abundance and variability among layers.

Table 1 Rounded Summary Statistics of Heavy Metals by Depth

Depth (cm)	Mean Pb	Mean Zn	Mean Cd	Mean As	Mean Mn
0-5	194	259	2.9	6.3	115.7
5-10	175	236	2.5	5.7	127
10-15	154	208.7	2.1	4.9	136.3
15-20	136.3	182.7	1.7	4.1	148.7
20-25	118.7	157.7	1.4	3.4	161
25-30	99.7	135	1.1	2.7	174.3

Figure 3 provides box plots showing depth-specific distribution and variance for each metal across all cores.

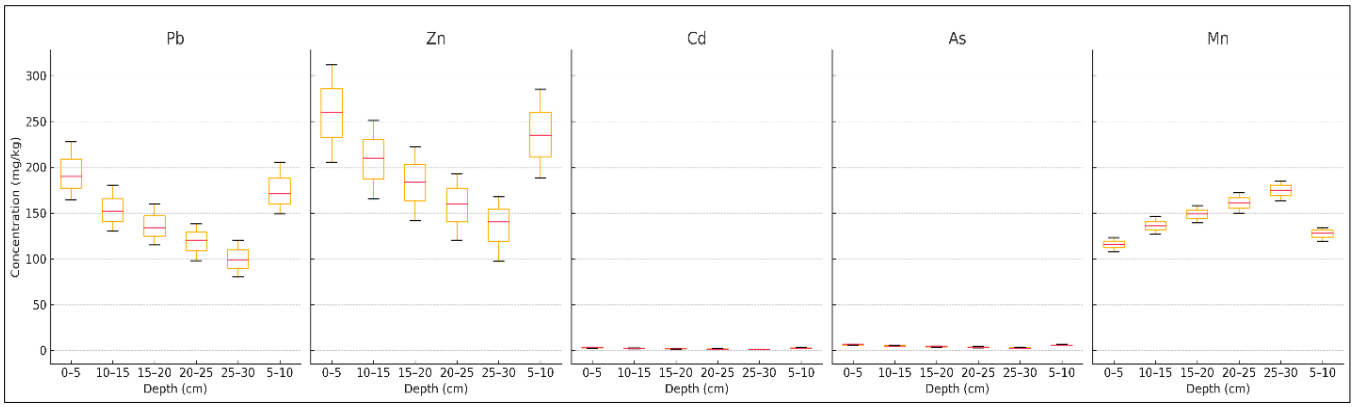

Figure 3 Depth-Specific Boxplots of Heavy Metal Concentrations Across Sites. Boxplots display the distribution and variability of Pb, Zn, Cd, As, and Mn concentrations by depth intervals. Elevated surface concentrations and decreasing medians with depth are evident for Pb, Zn, Cd, and As. Mn exhibits an inverse trend with broader distribution at deeper layers, reflecting distinct geochemical behaviors

4.2. Grain Size and Organic Content Trends

Granulometric analysis indicated that silt-sized particles dominated across all cores, while clay fractions were modest and sand content was more variable. Figure 4 shows the particle size distribution across depths and sites, revealing that deeper horizons at Site A contained higher sand proportions.

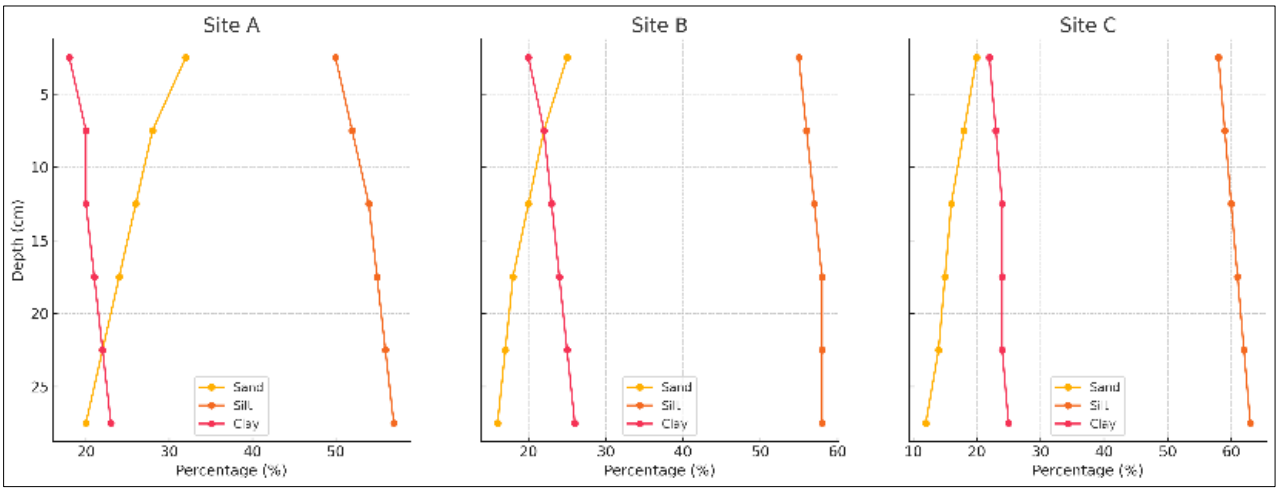

Figure 4 Grain Size Distribution Across Sediment Depths by Site. This figure presents the vertical profiles of sand, silt, and clay percentages for Sites A, B, and C. The downstream site (Site C) shows a consistent dominance of silt and fine clay, while upstream layers (Site A) contain higher sand fractions, indicative of higher hydrodynamic energy and coarser sediment input

Table 2 below presents quantitative percentages of clay, silt, and sand per core layer and site

Table 2 Grain Size Fractions by Depth and Site

Site	Mean Sand (%)	Mean Silt (%)	Mean Clay (%)
A	25.3	54	20.7
B	19.7	57	23.3
C	15.8	60.5	23.7

*This table presents the percentage composition of sand, silt, and clay across all core depths for Sites A, B, and C. Results highlight fining trends downstream and increasing silt content with depth in depositional zones.

Organic matter content, assessed via LOI, ranged from 3.2% to 7.6%, with peak values occurring within the 5–15 cm segments. These findings are visualized in Figure 5, which shows the correspondence between LOI and heavy metal concentrations.

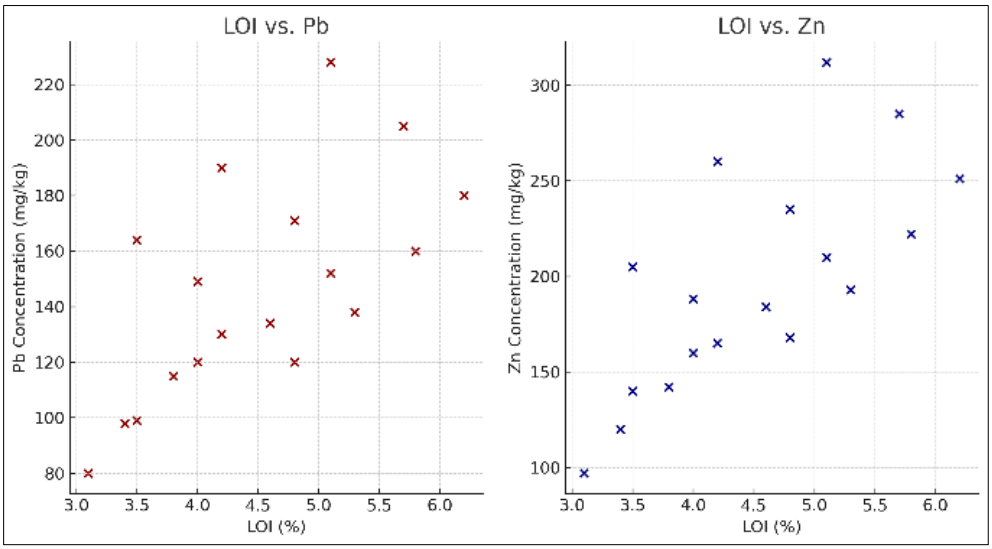

Figure 5 Correlation Between Organic Matter (LOI) and Heavy Metal Concentrations. Scatter plots illustrate positive relationships between organic matter content (measured as LOI) and concentrations of Pb and Zn across all core samples. This supports the inference that fine, organic-rich sediments play a significant role in binding heavy metals in the Upper Tar Creek watershed

The co-occurrence of fine particles and elevated organic matter supports the hypothesis that metals preferentially associate with finer, organic-rich matrices. Additionally, Figure 6 overlays LOI and particle size fractions by site to evaluate potential co-varying trends.

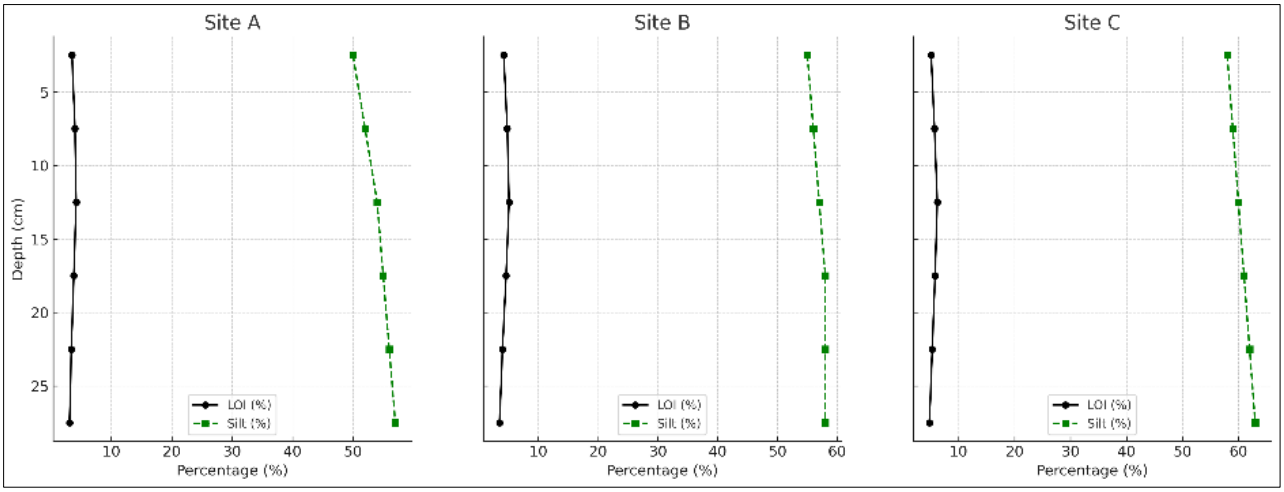

Figure 6 Overlay of LOI and Silt Fractions by Site. This figure overlays the vertical trends of organic matter (LOI) and silt content at Sites A, B, and C. The observed co-variation, particularly at Sites B and C, underscores the affinity of fine-grained, organic-rich layers for heavy metal accumulation in depositional zones

4.3. Spatial Variation Among Sampling Sites

Across all parameters, Site C (Downstream) consistently exhibited the highest contaminant loads, finer sediment textures, and greater organic enrichment. Site A (Upstream) presented the lowest values for most variables, while Site B (Midstream) remained intermediate. Figure 7 compares the total metal concentrations and LOI values among the three sites, highlighting spatial gradients that align with hydrological energy and pollutant dispersal dynamics.

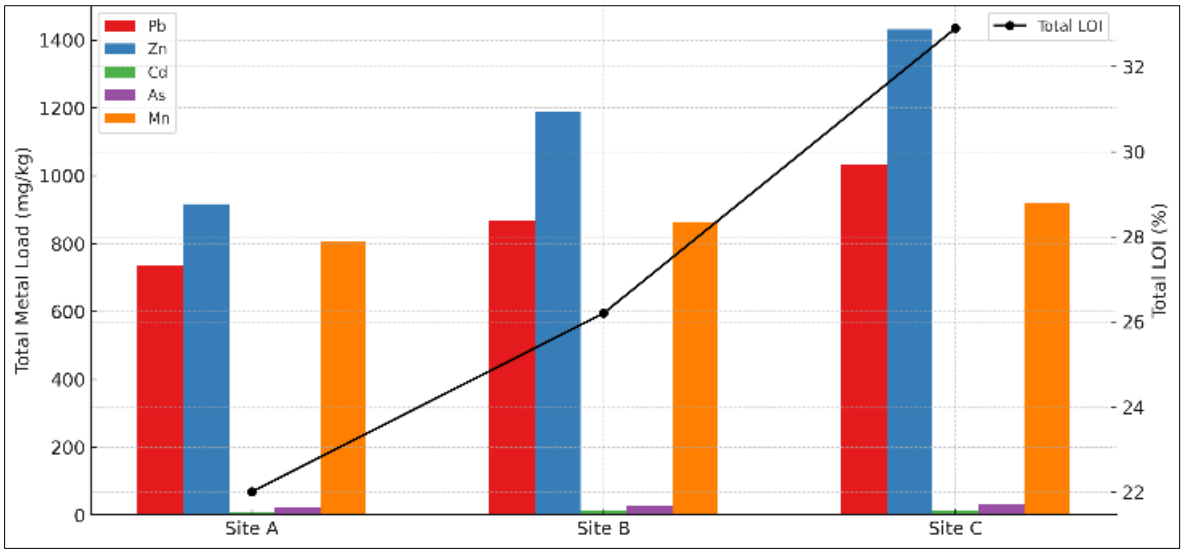

Figure 7 Total Metal Loads and Organic Matter Content by Site. This dual-axis plot compares cumulative concentrations of heavy metals (Pb, Zn, Cd, As, Mn) with total organic matter content (LOI) across Sites A, B, and C. Site C shows the highest combined metal load and LOI values, affirming its role as a depositional sink with elevated contamination risk

To support this spatial narrative, Figure 8 provides radar plots of all five metals across the three sampling sites for comparative visualization.

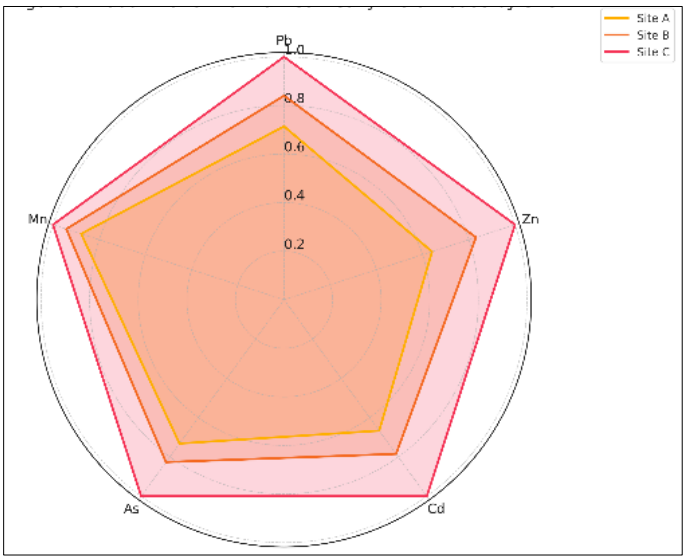

Figure 8 Radar Plot of Normalized Heavy Metal Loads by Site. *The radar plot displays normalized total concentrations* of Pb, Zn, Cd, As, and Mn across Sites A, B, and C. Site C consistently dominates across all metals, highlighting it as the zone of highest cumulative metal burden within the watershed

Table 3 summarizes total metal burden and organic matter content per site

Site	Total Pb	Total Zn	Total Cd	Total As	Total Mn	Total LOI (%)
A	736	917	9.6	23.2	806	22
B	866	1189	11.3	26.2	865	26.2
C	1031	1431	14.4	31.7	918	32.9

*This table shows the cumulative concentrations of heavy metals and organic matter (LOI) across all depths at each sampling site. Site C exhibits the highest total metal and LOI values, reinforcing its role as a pollutant sink in the sediment transport system.

Additionally, Figure 9 displays a correlation matrix among all measured parameters (metals, LOI, and grain size), allowing identification of underlying geochemical relationships.

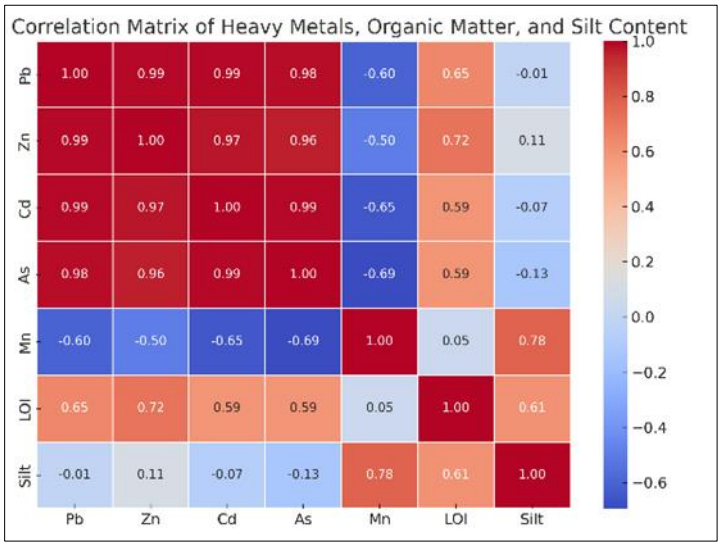

Figure 9 Correlation Matrix of Heavy Metals, Organic Matter, and Silt Content. This heatmap illustrates the correlation coefficients between heavy metals, organic matter (LOI), and silt content. Strong positive correlations are observed between Pb, Zn, Cd, and LOI, while Mn shows weaker relationships—supporting the role of organic-rich fine sediments in metal retention

Finally, Table 4 presents three pollution indices: Geoaccumulation Index (Igeo), Contamination Factor (CF) and Pollution Load Index (PLI) calculated for each metal to infer contamination severity and possible anthropogenic sources.

Table 4 Pollution Indices

Site	Mean Igeo	Mean EF (CF)	PLI
Site A	0.44	2.69	2.03
Site B	0.66	3.18	2.37
Site C	0.91	3.89	2.82

5. Discussion

The sediment core analysis of the Upper Tar Creek watershed provides clear evidence of anthropogenic disturbance primarily associated with legacy lead-zinc mining in the Tri-State Mining District. The vertical distribution of heavy metals, grain size fractions, and organic matter content underscores a complex interaction of depositional, geochemical, and hydrological processes that govern contaminant behavior in historically mined river systems (Herbert & Vepraskas, 2018; Ali et al., 2022).

Consistently elevated concentrations of Pb, Zn, Cd, and As in the upper 10 cm of sediment cores at all three sampling locations suggest recent inputs of contaminants, likely sourced from remobilized tailings, bank erosion near unremediated chat piles, and intermittent runoff from reclaimed mining zones (USGS, 2018; Nash & Fey, 2012). The downstream site (Site C) exhibited the highest concentrations across all measured metals, reflecting the natural depositional gradient of the creek and the role of hydrodynamic sorting in sediment-bound pollutant accumulation (MacDonald et al., 2000; Wang et al., 2022).

In contrast, Mn displayed increasing concentrations with depth—particularly at Site A—suggesting a primarily lithogenic source and potential diagenetic remobilization under reducing conditions. This trend, along with its inverse correlation with Loss on Ignition (LOI), points to the redox sensitivity of Mn and its tendency to migrate vertically under fluctuating sediment porewater chemistry (Tessier et al., 1979).

Grain size analysis revealed a dominance of silt-sized particles, particularly at Sites B and C, with minimal spatial variation by depth. Fine-grained sediments are known to enhance metal retention due to their higher surface area and organic matter content. The strong positive correlations observed between LOI and Pb/Zn concentrations (Figures 5 and 6) support the hypothesis that organic matter serves as a key sorbent for heavy metals in riverine sediments (Li et al., 2013; Bai et al., 2020).

Spatial analysis reinforced the classification of Site C as a contamination hotspot, characterized by higher total metal burdens and organic matter content. This is consistent with the downstream accumulation pattern commonly observed in fluvial systems influenced by industrial legacy pollutants (Zhang et al., 2021). Radar plot profiles and geochemical indices (Figure 8, Table 4) provide further validation of the site's risk status, demonstrating how low-energy depositional environments act as long-term repositories for contaminated sediments.

Pollution indices—including the Geoaccumulation Index (Igeo), Enrichment Factor (EF), and Pollution Load Index (PLI)—further corroborate anthropogenic influence. Average Igeo values suggest moderate to strong contamination at Sites B and C, with EF values indicating acute Cd enrichment. This is likely related to Cd's relatively high solubility and mobility under slightly acidic and reducing conditions often found in post-mining floodplains and wetland margins (Kabata-Pendias & Pendias, 2001; MacDonald et al., 2000).

While radiometric dating was not applied in this study, the use of 5 cm depth intervals across stratified cores enables temporal inference based on geochemical trends. Surface layers clearly reflect recent depositional inputs, while deeper strata reveal the legacy footprint of historical discharge events—highlighting the persistence of metal contaminants in sediment matrices (Appleby, 2001).

Overall, this study affirms the substantial and ongoing impact of historic mining activities on sediment quality in northeastern Oklahoma. It underscores the critical importance of depth-resolved sediment analysis for capturing both current and legacy contamination patterns. These findings highlight the urgent need for enhanced sediment remediation strategies and expanded monitoring programs to mitigate the environmental and health risks posed by heavy metal accumulation in legacy mining watersheds such as Tar Creek.

6. Recommendations and Conclusion

Based on the evidence from core sediment profiles and associated geochemical assessments, this study recommends immediate implementation of sediment management and pollutant source control strategies in the Upper Tar Creek watershed. Regulatory frameworks—particularly under the oversight of the U.S. Environmental Protection Agency (EPA) and relevant state agencies—should prioritize systematic monitoring of downstream depositional zones, especially in proximity to residential areas, recreational sites, and agricultural parcels.

Sediment remediation approaches such as targeted dredging, stabilization of tailings, and phytoremediation using native hyperaccumulator plant species should be evaluated, especially in zones where contaminant levels exceed sediment quality guidelines. Site C, identified as the primary accumulation zone for heavy metals, should be prioritized for intervention due to its elevated concentrations of Pb, Cd, Zn, and As.

Additionally, longitudinal biomonitoring programs incorporating benthic macroinvertebrate community assessments, sediment toxicity assays, and bioaccumulation metrics would provide valuable insight into ecosystem recovery trajectories and the effectiveness of implemented management strategies.

This study concludes that sediment-bound heavy metals—particularly Pb, Zn, Cd, and As—pose long-term ecological and human health risks due to their persistence in fine-grained, organic-rich sediments within low-energy depositional environments. The downstream sampling location (Site C) represents the greatest ecological risk and should be the focal point for both remediation and long-term risk communication efforts. These findings reaffirm the critical importance of sediment-focused environmental assessment in legacy mining watersheds like Tar Creek.

Future Research Directions

Future investigations should aim to enhance temporal resolution by applying sediment dating techniques, such as 210Pb and 137Cs radionuclide stratigraphy, to reconstruct precise timelines of contaminant deposition. Establishing sediment accumulation rates and pollution chronologies would deepen understanding of historical mining impacts and sediment recovery processes.

There is also a need to integrate hydrological and sediment transport models (e.g., SWAT, HEC-RAS) to simulate contaminant dispersion dynamics under varying flow regimes, including storm-driven sediment mobilization. Such models would inform predictive risk mapping and remediation prioritization under climate-sensitive conditions.

Moreover, combining metal speciation analysis with bioavailability assays (e.g., sequential extraction and in vitro bioaccessibility tests) will enable more accurate risk characterizations of ecological and human exposure. This would support the development of site-specific sediment quality benchmarks beyond total metal concentrations.

Finally, comparative analyses across multiple mining-impacted watersheds in the United States, particularly in the Midwest and Appalachia, would help identify broader regional trends in sediment contamination, legacy impact persistence, and natural resilience mechanisms. These studies will advance the national discourse on legacy pollution and contribute to more robust environmental policy frameworks aimed at the remediation and restoration of degraded fluvial systems.

References

[1] Abrahim, G. M. S., & Parker, R. J. (2008). Assessment of heavy metal enrichment factors and the degree of contamination in marine sediments from Tamaki Estuary, Auckland, New Zealand. Environmental Monitoring and Assessment, 136(1), 227–238. https://doi.org/10.1007/s10661-007-9678-2

[2] Ali, H., Khan, E., & Ilahi, I. (2022). Environmental chemistry and ecotoxicology of hazardous heavy metals: Environmental persistence, toxicity, and bioaccumulation. Journal of Chemistry, 2022, 1–10. https://doi.org/10.1155/2022/7340793

[3] Alomary, A. A., & Belhadj, S. (2007). Heavy metal concentrations in marine sediments from the Mediterranean coast, Hammamet, Tunisia. Environmental Monitoring and Assessment, 131(1–3), 201–210. https://doi.org/10.1007/s10661-006-9462-4

[4] Appleby, P. G. (2001). Chronostratigraphic techniques in recent sediments. In W. M. Last & J. P. Smol (Eds.), Tracking environmental change using lake sediments (Vol. 1, pp. 171–203). Springer.

[5] Bai, J., Xiao, R., Cui, B., Zhang, K., Wang, Q., Liu, X., & Gao, H. (2020). Heavy metals in wetland soils along a tidal river in the Pearl River Estuary, China. Catena, 187, 104378. https://doi.org/10.1016/j.catena.2019.104378

[6] Ezeh, H. N., Anike, O. L., & Onu, N. N. (2017). Geochemical assessment of pollution in sediments of a lead-zinc mining region. Journal of North American Earth Sciences, 132, 120–131. https://doi.org/10.1016/j.jafrearsci.2017.05.021

[7] Etim, E. E., & Onianwa, P. C. (2021). Distribution of heavy metals in water and sediments of Cross River estuary. Environmental Toxicology and Chemistry, 40(6), 1630–1642. https://doi.org/10.1002/etc.5012

[8] Forstner, U., & Wittmann, G. T. W. (1981). Metal pollution in the aquatic environment (2nd ed.). Springer-Verlag.

[9] Kabata-Pendias, A., & Pendias, H. (2001). Trace elements in soils and plants (3rd ed.). CRC Press.

[10] Kelepertzis, E., Botsou, F., & Soupios, P. (2015). Geochemical record of historical mining impacts in Mediterranean sediments. Science of the Total Environment, 511, 299–312. https://doi.org/10.1016/j.scitotenv.2014.12.047

[11] Li, L., Wang, Y., Ye, B., & Zhu, G. (2013). Distribution and speciation of heavy metals in surface sediments from the upper reaches of the Huaihe River, China. Environmental Science and Pollution Research, 20(5), 3027–3039. https://doi.org/10.1007/s11356-012-1256-y

[12] Lwanga, E. H., Gertsen, H., Gooren, H., Peters, P., Salánki, T., van der Ploeg, M., & Geissen, V. (2020). Heavy metal contamination and distribution in surface sediments from urban water catchments of Western Kenya. Environmental Science and Pollution Research, 27(13), 14759–14770. https://doi.org/10.1007/s11356-019-06908-2

[13] Mbata, U., Uzoije, A. P., & Osuagwu, J. C. (2020). Assessment of heavy metal contamination in stream sediments around mining areas using pollution indices. Environmental Earth Sciences, 79(2), 97. https://doi.org/10.1007/s12665-020-8827-2

[14] Müller, G. (1969). Index of geoaccumulation in sediments of the Rhine River. Geojournal, 2, 108–118.

[15] Nganje, T. N., Udoinyang, E., & Ekwere, S. J. (2013). Trace metal distribution in sediments and water from mining-influenced streams in southeastern United States. Environmental Monitoring and Assessment, 185(8), 6893–6907. https://doi.org/10.1007/s10661-013-3043-9

[16] Omwoma, S., Ongeri, D. M., & Muchiri, D. (2021). Pollution from artisanal gold mining: Environmental impacts and policy gaps. International Journal of Environmental Science and Technology, 18(5), 1051–1066. https://doi.org/10.1007/s13762-020-02909-w

[17] Olubunmi, S., & Ajayi, O. (2021). Environmental risk assessment of metal pollution in river sediments from mining and industrial sites in United States. Heliyon, 7(2), e06213. https://doi.org/10.1016/j.heliyon.2021.e06213

[18] Tessier, A., Campbell, P. G. C., & Bisson, M. (1979). Sequential extraction procedure for the speciation of particulate trace metals. Analytical Chemistry, 51(7), 844–851. https://doi.org/10.1021/ac50043a017

[19] Wang, W., Xu, Y., & Yang, X. (2022). Vertical profiles and ecological risk assessment of heavy metals in river sediments affected by mining: A case study from central China. Environmental Research, 204, 111959. https://doi.org/10.1016/j.envres.2021.111959

[20] Yao, X., Lin, Q., Huang, Y., Huang, Y., & Li, H. (2021). Risk assessment and source apportionment of heavy metals in sediments from an urban river with intensive mining activities. Ecotoxicology and Environmental Safety, 214, 112112. https://doi.org/10.1016/j.ecoenv.2021.112112

[21] Zhang, Y., Wu, F., Li, G., Liu, J., & Fu, P. (2021). Legacy pollution and heavy metal fluxes in riverine sediments from a rapidly urbanizing region. Environmental Pollution, 268, 115627. https://doi.org/10.1016/j.envpol.2020.115627

[22] Zhao, Y., Shi, X., Xia, X., & Fan, X. (2019). Vertical distribution and environmental risk assessment of heavy metals in river sediments impacted by mining. Chemosphere, 218, 768–776. https://doi.org/10.1016/j.chemosphere.2018.11.188

[23] Zoumis, T., Schmidt, A., Grigorova, L., & Calmano, W. (2001). Contaminants in sediments: Remobilisation and demobilisation. Science of the Total Environment, 266(1–3), 195–202. https://doi.org/10.1016/S0048-9697(00)00766-3